Macromolecules
ARTICLE

Macromolecules **2010**, *43*, 6085–6091 **6085**
DOI: 10.1021/ma1011182

Enhancement of P3HT/PCBM Photovoltaic Efficiency Using the Surfactant of Triblock Copolymer Containing Poly(3-hexylthiophene) and Poly(4-vinyltriphenylamine) Segments

Jung-Hsun Tsai,[†,‡] Yi-Cang Lai,[§,‡] Tomoya Higashihara,*[,∥] Chih-Jung Lin,[†] Mitsuru Ueda,*[,∥] and Wen-Chang Chen*[,†,§]

[†]*Department of Chemical Engineering, National Taiwan University, Taipei, Taiwan 106,* [§]*Institute of Polymer Science and Engineering, National Taiwan University, Taipei, Taiwan 106, and* [∥]*Department of Organic and Polymeric Materials, Tokyo Institute of Technology, 2-12-1 Ookayama, Meguro-ku, Tokyo 152-8552, Japan.* [‡]*J. H. Tsai and Y. C. Lai equally contributed to this work*

Received May 20, 2010; Revised Manuscript Received June 11, 2010

ABSTRACT: In this study, the well-defined coil−rod−coil triblock copolymer poly(4-vinyltriphenylamine)-*b*-poly(3-hexylthiophene)-*b*-poly(4-vinyltriphenylamin) (**PTPA-P3HT-PTPA**) was used as a surfactant for P3HT/PCBM (1:1) based solar cells. The power conversion efficiency of the device was enhanced from 3.9 to 4.4% in the presence of the 0−5% **PTPA-P3HT-PTPA** under illumination of AM 1.5G (100 mW/cm^2). The morphology variation and the balance of the hole/electron mobility accounted for such enhancement. In the P3HT/PCBM/**PTPA-P3HT-PTPA** ternary blends, the fiber-like structure was observed for surfactant ratios of 0−5%, while a sphere-like nanostructure was observed for the surfactant ratio of 1.5%. The sphere-like nanostructure led to a smaller domain size and enhanced interfacial area for charge separation as compared to the fiber-like structure. On the other hand, the increased hole mobility in the blend with the addition of **PTPA-P3HT-PTPA** resulted in the balanced hole and electron mobility ($\mu_e/\mu_h \sim 1.7$ in comparison to the ratio of 3.6 without the surfactant). The incorporated **PTPA-P3HT-PTPA** surfactant not only extended the lifetime of solar cells but also reduced the PCBM aggregation upon annealing, resulting in better thermal stability. The DSC result confirmed the selective miscibility of the PTPA coil segment with PCBM. These results demonstrated the superior compatibilizing effect of the rod−coil triblock copolymers for solar cell applications.

Introduction

Polymer bulk-heterojunction (BHJ) solar cells with a photoactive layer consisting of an interpenetrating network of π-conjugated polymer donors and soluble fullerene or nanocrystal acceptors, have attracted much interest because of their easy processability, low material cost, high efficiency, and mechanical flexibility.[1−14] The most used system up to now is a blend of regioregular poly(3-hexylthiophene) (rr-P3HT) and [6,6]-phenyl-C_{61}-butyric acid methyl ester (PCBM), in which well-acknowledged state-of-the-art P3HT/PCBM BHJ solar cells give efficiencies in the range of 3−5%.[2,6,7] In such blend materials, the typical exciton diffusion length of conjugated polymers is about 10 nm, therefore the donor and acceptor materials should ideally form 10 nm-scale interpenetrating networks within the active layer to ensure an efficient dissociation of excitons.[15,16] Control of the morphology within the BHJ active layer, including different solvents (or mixed solvents),[17] solvent annealing,[2,6] processing additives,[3,18−22] and thermal treatment,[7,23] could significantly facilitate nanoscale phase separation and further enhance the device performance. For a P3HT/PCBM blend, the crystallized P3HT fibril structure and enhanced charge transport was found via a thermal annealing process; however, the phase segregation of the active layer changes dramatically upon heating owing to the aggregation and diffusion of PCBM clusters.[7,23] The phase separation decreases the interfacial area and causes insufficient exciton dissociation between P3HT and PCBM.

*To whom all correspondence should be addressed. E-mail: (M.U.) ueda.m.ad@m.titech.ac.jp; (W.-C.C.) chenwc@ntu.edu.tw; (T.H.) thigashihara@polymer.titech.ac.jp.

Recently, rod−coil copolymers containing P3HT segments have been designed for optoelectronic devices due to their tunable morphology.[24−30] McCullough et al. reported the synthesis of P3HT-coil based block copolymers with the hole mobility as high as 0.05 cm^2 V^{-1} s^{-1}.[26,27,29,39,40] Also, Thelakkat et al. applied the double-crystalline donor−acceptor block copolymer, P3HT-*b*-poly(perylene bisimide acrylate), to single-layer solar cells.[24,25] Another novel approach is to apply these rod−coil copolymers to a "surfactant" for solar cell device applications.[18−22] Fréchet et al. first employed a donor−acceptor diblock copolymer as a surfactant not only to tune the device morphology but also to stabilize the device structure against destructive thermal phase segregation.[18] In addition, the harmonizing effect of the diblock copolymer on a P3HT/perylene bisimide-based device has been explored for controlling the phase separation within the active layer.[19] Wudl and co-workers reported that the addition of 5 wt % P3HT-based copolymers resulted in an improved performance (PCE = 3.5%), higher than that obtained from a pristine P3HT/PCBM device (PCE = 2.6%).[21] However, the synthetic methods for such block copolymers include complicated multistep reactions. In addition, there has never been a report on a photovoltaic application achieving more than 4% based on a surfactant approach employing block copolymers.

Our group has developed a facile synthetic methodology for coil−rod−coil triblock copolymers with low polydispersities (PDI < 1.2) by a combination of quasi-living Grignard metathesis and living anionic polymerizations,[31,32] as shown in Scheme 1. Our goal in this study is to incorporate different ratios of poly(4-vinyltriphenylamine)-*b*-poly(3-hexylthiophene)-*b*-poly(4-vinyltriphenylamine) (**PTPA-P3HT-PTPA**) into P3HT/PCBM-based

Published on Web 06/17/2010

devices serving as a surfactant. The motivations for the selection of PTPA are as follows. (1) **PTPA-P3HT-PTPA** itself showed a clear microphase separation with a neat and periodic lamellar morphology of 10−12 nm in width, comparable to an exciton diffusion length.[32] (2) PTPA is an amorphous coil-like polymer, so PCBM may be selectively miscible with the PTPA domain rather than the crystalline P3HT domain. (3) The hole-transporting property of PTPA does not interfere significantly with the hole mobility of P3HT compared to completely insulating coil polymers like PS and PMMA segments. The effects of different block copolymer ratios on optical properties, morphology, thermal properties, and field effect transistor (FET) characteristics were studied and correlated to the solar cell performance. The experimental results suggested that the improved PCE of a P3HT/PCBM solar cell device achieving 4.4% and enhanced long-term stability upon heating could be attributed to the change of morphology and superior compatibilizing effect with the introduction of triblock copolymer, **PTPA-P3HT-PTPA**.

Scheme 1. Synthetic Routes for the Studied Coil−Rod−Coil Triblock Copolymer PTPA-P3HT-PTPA

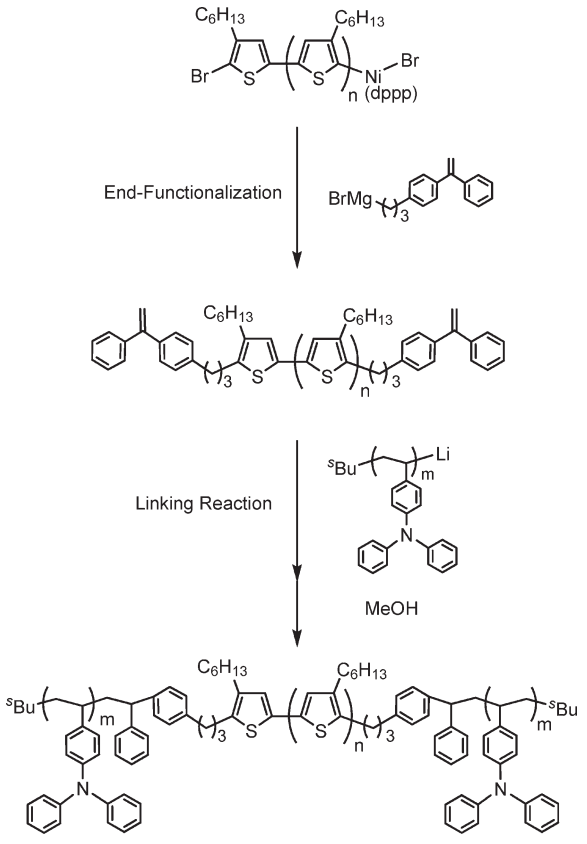

PTPA-P3HT-PTPA

Experimental Section

Materials. A triblock copolymer, **PTPA-P3HT-PTPA**, was successfully synthesized via well-controlled living anionic polymerization, as illustrated in Scheme 1.[32] The number-average molecular weight (M_n) of **PTPA-P3HT-PTPA**, estimated by GPC, was around 27000 g/mol with a polydispersity index (PDI) value of 1.17. The average molecular weight of different segments of the triblock copolymer, estimated from the ^{1}H NMR spectrum, was 8480−10000−8480 (**PTPA-P3HT-PTPA**) g/mol. Commercial P3HT (M_n = 25000 g/mol, PDI ∼ 2, regioregularity ∼98.5%) and PCBM were obtained from Rieke-Metal and Nano-C, respectively. The ultra-anhydrous solvents and common organic solvents were purchased from Tedia, Merck, and J. T. Baker. All reagents were used as received.

Preparation of Polymer Blends and Their Characterization. Different ratios of surfactant (0−20 wt % with respect to the amount of P3HT/PCBM, as listed in Table 1), **PTPA-P3HT-PTPA**, were blended into P3HT/PCBM in *o*-dichlorobenzene (*o*-DCB) to form homogeneous solutions. They were then filtered through syringe filters with PTFE membrane (0.45 μm pore size), then spin-coated at a speed rate of 450 rpm for 60 s onto the quartz substrate, and annealed for 20 min at 140 °C. UV−Vis absorption spectra of the spin-coated blended films on quartz substrates were recorded on a Hitachi U-4100 spectrophotometer. Atom force microscopy (AFM) measurements were obtained with a 3D Controller AFM (Digital Instruments, Santa Barbara, CA) operated in a tapping mode at room temperature. Commercial silicon cantilevers (Nanosensors, Germany) with typical forced constants of 5−37 N m-1 was used. Images were taken continuously with the scan rate of 1.0 Hz. The film thickness values were measured using a profilometer (Surfcorder ET3000).

Fabrication and Characterization of Polymer Solar Cells. All the bulk-heterojunction photovoltaic cells were prepared using the same preparation procedures and device fabrication procedure referring as follows: The glass-indium tin oxide (ITO) substrates (obtained from Lumtec, (7 Ω/sq) were first patterned by lithograph, then cleaned with detergent, and ultrasonicated in acetone and isopropyl alcohol, and subsequently dried on a hot plate at 120 °C for 5 min, and finally treated with oxygen plasma for 5 min. Poly(3,4-ethylenedioxy−thiophene):poly(styrene−sulfonate) (PEDOT:PSS, Baytron P VP AI4083) was passed through a 0.45 μm filter before being deposited on ITO with a thickness around 30 nm by spin coating at 5000 rpm in the air and dried at 140 °C for 20 min inside glovebox. The blended film of the P3HT:PCBM/**PTPA-P3HT-PTPA** in *o*-DCB were spin-coated at a speed rate of 450 rpm for 60 s on the top of PEDOT:PSS layer. These films were kept in covered Petri dish with drilling holes in order to control drying rate. After that, the devices were annealing at 140 °C for 20 min in glovebox. Subsequently the device was completed by thermal evaporation

Table 1. Photovoltaic and FET Characteristics of the Studied P3HT/PCBM (1:1, w/w) Blended with Different Ratios of PTPA-P3HT-PTPA as Surfactant

	FET mobility			solar cell P3HT/PCBM (1:1)			
additives of PTPA-P3HT-PTPA (%)	hole (μ_h) ($cm^2V^{-1}s^{-1}$)	electron (μ_e) ($cm^2V^{-1}s^{-1}$)	μ_e/μ_h (−)	J_{sc} (mA/cm^2)	V_{oc} (V)	FF (−)	PCE (%)
0	7.17×10^{-4}	2.58×10^{-3}	3.6	9.7	0.62	0.65	3.9
0.25	7.41×10^{-4}	1.81×10^{-3}	2.4	9.7	0.62	0.65	3.9
0.5				10.4	0.62	0.62	4.0
1				10.8	0.61	0.63	4.2
1.5	8.89×10^{-4}	1.52×10^{-3}	1.7	11.2	0.62	0.63	4.4
2.5				10.6	0.63	0.64	4.2
5	1.50×10^{-3}	1.95×10^{-3}	1.3	10.9	0.62	0.62	4.2
10				10.0	0.61	0.60	3.6
20				8.4	0.63	0.60	3.0

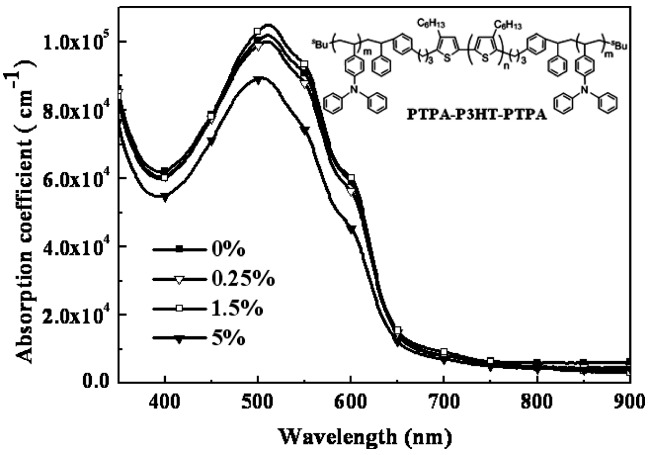

Figure 1. Optical absorption spectra of the P3HT/PCBM (1:1, w/w) blended with 0%, 0.25%, 1.5%, and 5% of **PTPA-P3HT-PTPA** in thin films on quartz plate using *o*-dichlorobenzene as the processing solvent.

of Ca (30 nm) and Al (100 nm) under $< 10^{-6}$ Torr pressure. The active area of the device is 4 mm^2. The current−voltage ($I-V$) measurement of the polymer photovoltaic cells was conducted by a computer-controlled Keithley 2400 source measurement unit (SMU) with a Peccell solar simulator under the illumination of AM 1.5G, 100 mW/cm^2. The illumination intensity was calibrated by a standard Si photodiode detector with KG-5 filter.

Fabrication and Characterization of Thin Film Transistors. Highly doped *n*-type Si (100) wafers were used as substrates. A 300 nm SiO_2 layer (capacitance per unit area C_i = 10 nF cm^{-2}) as a gate dielectric was thermally grown onto the Si substrates. These wafers were cleaned in piranha solution, a 7:3 mixture of H_2SO_4 and H_2O_2, rinsed with deionized water, and then dried by N_2. Then, the substrates were rinsed with toluene, acetone, isopropyl alcohol, and dried with a steam of nitrogen. The spin-coated films of P3HT/PCBM (1:1) blended with various amounts of **PTPA-P3HT-PTPA** (0%, 0.25%, 1.25%, and 5%) were prepared from *o*-DCB solutions at a spin rate of 450 rpm for 60 s. These films were kept in covered Petri dish with drilling holes in order to control drying rate. After drying, these samples were kept for 20 min at 140 °C to anneal. The top-contact source and drain electrodes were defined by 100 nm thick gold through a regular shadow mask, and the channel length (L) and width (W) were 50 and 1000 μm, respectively. OTFT transfer and output characteristics were recorded in a N_2-filled glovebox or in ambient by using a Keithley 4200 semiconductor parameter analyzer.

Results and Discussion

Optical properties. Figure 1 shows the UV−vis absorption spectra of P3HT/PCBM (1:1) films blended with different ratios of **PTPA-P3HT-PTPA** cast from *o*-DCB and annealed at 140 °C for 20 min in glovebox. With the addition of the triblock copolymer, the blended films exhibit similar absorption spectra when compared to pristine P3HT/PCBM film. In general, the three distinct absorption peaks could be attributed to the $\pi-\pi^*$ transition (511 nm) and $\pi-\pi$ stacking (555 and 605 nm) of P3HT.[33] Comparable absorption intensities of blend films containing 0%, 0.25%, and 1.5% **PTPA-P3HT-PTPA**, obtained at around 1.00×10^5 to 1.05×10^5 cm^{-1} (at an absorption maximum of 605 nm), indicate that small amounts of **PTPA-P3HT-PTPA**, incorporated into the P3HT/PCBM system, do not affect significantly the crystallinity of P3HT. However, with the addition of 5% **PTPA-P3HT-PTPA**, the absorption coefficient apparently decreases, which not only decreases the absorptivity but also affects the packing of P3HT.

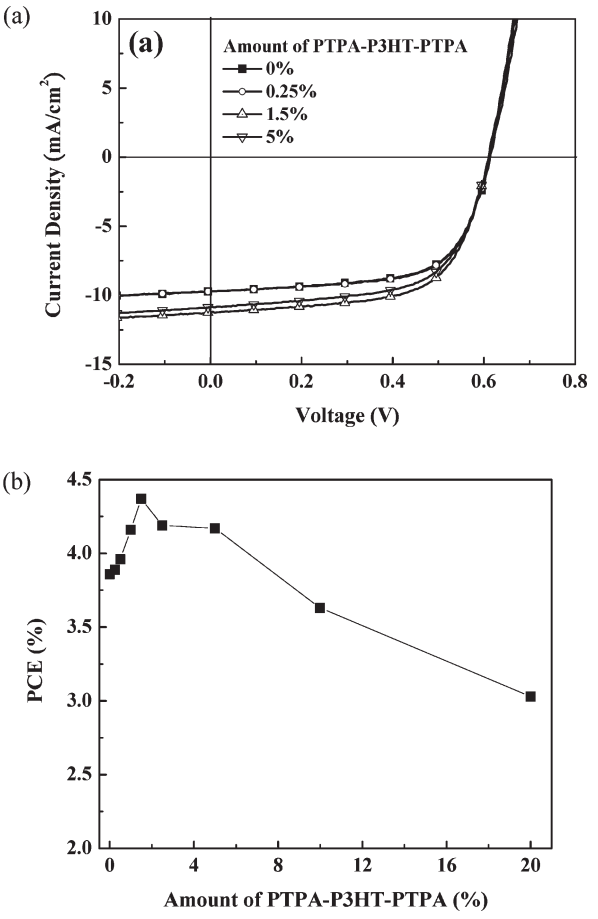

Figure 2. (a) $I-V$ characteristics of polymer solar cells with P3HT/PCBM (1:1, w/w) with the addition of 0%, 0.25%, 1.5%, and 5% **PTPA-P3HT-PTPA** under the illumination of AM 1.5G, 100 mW/cm^2. (b) PCE of P3HT/PCBM (1:1, w/w) blended with different ratios of **PTPA-P3HT-PTPA**.

Photovoltaic Cell Characteristics. The bulk heterojunction solar cells were fabricated with layer-by-layer structure of glass/ITO/PEDOT:PSS/P3HT:PCBM (1:1 w/w):**PTPA-P3HT-PTPA**/Ca (30 nm)/Al (100 nm). $I-V$ characteristics and the related parameters of P3HT/PCBM solar cells blend with different ratios of **PTPA-P3HT-PTPA** are shown in Figure 2a and summarized in Table 1. The PCE (%) of the corresponding polymer of various ratios of **PTPA-P3HT-PTPA** in P3HT/PCBM (1:1) system are 3.9 (0%), 3.9 (0.25%), 4.0 (0.5%), 4.2 (1%), 4.4 (1.5%), 4.2 (2.5%), 4.2 (5%), 3.6 (10%), and 3.0 (20%), respectively, as depicted in Figure 2(b). Obviously, the enhanced PCE as compared to the pristine P3HT/PCBM system could be related to the addition of the surfactant.

As listed in Table 1, where the V_{oc} values of the photovoltaic devices are maintained in the range of 0.61−0.63 V indicates that the small amounts of **PTPA-P3HT-PTPA** do not affect the HOMO level of the P3HT-based donor system. With similar absorption ability and molecular energy levels of the P3HT/PCBM/**PTPA-P3HT-PTPA** system described above, we could attribute the enhanced PCE to the charge transport mobility and morphology, as analyzing the following sections.

Field Effect Transistors (FETs) Characteristics. Since the charge transport in polymer blends is crucial for solar cells, the FET is a powerful tool to investigate the hole and electron mobilities of polymer blends.[34] All FET devices were fabricated by employing top-contact configuration for

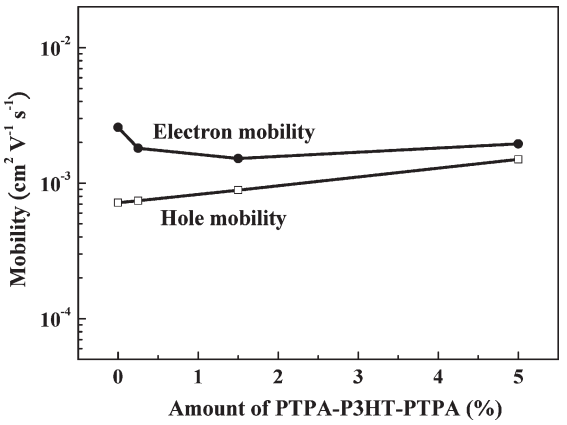

Figure 3. Hole/electron mobilities in the P3HT:PCBM (1:1, w/w) blended with 0%, 0.25%, 1.5%, and 5% of **PTPA-P3HT-PTPA**.

reducing contact resistance. In order to understand the balance between hole and electron mobilities within polymer blends and its effect on solar cell performance, we used a bare Si/SiO_2 wafer without any surface treatment for preventing the vertical segregation of PCBM.[35] The transfer characteristics of the studied blended materials based FET devices are shown in Figure S3 of the Supporting Information. The saturation-regime mobility was estimated from the slope of the plot of drain-to-source current $(I_d)^{1/2}$ as a function of the gate voltage (V_g).[38] FET devices based on the spin-coated films of P3HT/PCBM (1:1) blended with various amounts of **PTPA-P3HT-PTPA** (0%, 0.25%, 1.25%, and 5%) were fabricated and the corresponding carrier mobilities are listed in Table 1 and depicted in Figure 3. The μ_h of the P3HT/PCBM system with various amounts of **PTPA-P3HT-PTPA** are 7.17×10^{-4} (0%), 7.41×10^{-4} (0.25%), 8.89×10^{-4} (1.5%), and 1.50×10^{-3} (5%) cm2 V^{-1} s^{-1}, respectively, while their corresponding μ_e are 2.58×10^{-3}, 1.81×10^{-3}, 1.52×10^{-3}, and 1.95×10^{-3} cm^2 V^{-1} s^{-1}, respectively. The highest μ_e/μ_h ratio (3.6) of pristine P3HT/PCBM (1:1) is similar to a previous work with a space-charge-limited current (SCLC) model.[36] The higher electron mobility compared to the hole mobility is due to the intrinsic electron-transport and easily percolated network characteristics of PCBM. In our case, the hole mobility increases gradually which may be due to the donor characteristic of **PTPA-P3HT-PTPA**,[32] further reducing the μ_e/μ_h ratio with the addition of the surfactant. Note that the low μ_e/μ_h ratio of 1.5% (1.7) and 5% (1.3) **PTPA-P3HT-PTPA** blended system could be achieved, and a balanced mobility is crucial for high-performance solar cell applications.

Atom Force Microscopy (AFM) measurement was explored to further investigate the molecular organization and film morphology of the blended system. Figure 4 and Figure S3 (in Supporting Information) show the AFM images of the P3HT/PCBM (1:1, w/w) system with different ratios of **PTPA-P3HT-PTPA**. The fiber-like structure could be observed with the addition ratios ranging from 0% to 1%. Interestingly, a sphere-like structure was found by adding 1.5% **PTPA-P3HT-PTPA**, as shown in Figure 4b. By further increasing the addition ratios from 2% to 5%, the morphology changes from sphere to fiber, which suggests that the formation of a smaller domain size of sphere-like conformations could enhance the interfacial area in comparison to the fibrous structure. Furthermore, with the balanced mobilities of charge transport (μ_e/μ_h ~1.7), the highest J_{sc} (11.2 mAcm-2) of the 1.5% **PTPA-P3HT-PTPA** blended system could be reached in accordance with the above two

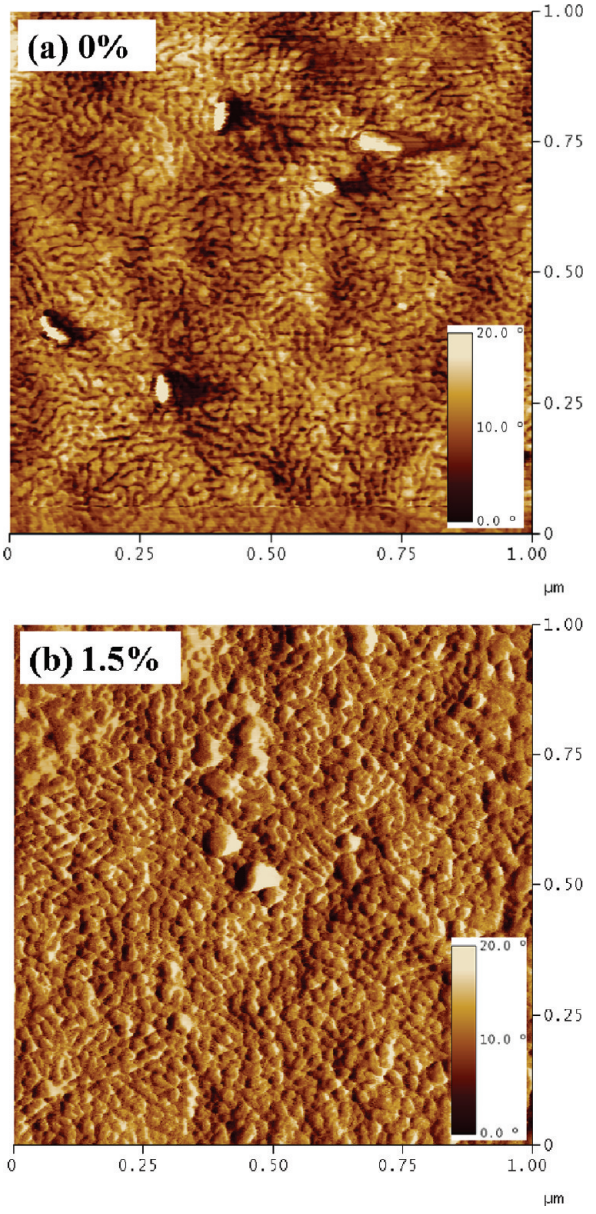

Figure 4. AFM phase images of the P3HT/PCBM (1:1, w/w) with (a) 0% and (b) 1.5% **PTPA-P3HT-PTPA** cast from *o*-dichlorobenzene. The image sizes are all 1 μm × 1 μm and the *Z* range is 20°.

factors. Even more balanced mobilities (μ_e/μ_h ~1.3) were obtained using 5% **PTPA-P3HT-PTPA** compared to 1.5%, however the absorption ability was reduced seriously as the higher insulating segments were introduced. Hence, the best device performance was achieved with a V_{oc} of 0.62 V, J_{sc} of 11.2 mA/cm^2, fill factor of 0.63, and PCE of 4.4% when 1.5% **PTPA-P3HT-PTPA** was used. A PCE of 4.4% has never been reached in a system employing block copolymers as surfactants.

Longevity and Thermal Stability of Photovoltaic Cells. Apart from the efficiency improvement, air stability is another critical issue for photovoltaic cells. When oxygen and humidity are present, their diffusion into the cells is generally regarded as the dominant source of degradation. Protection of solar cells from air and humidity is necessary to extend their lifetime. To investigate the air stability for a device's lifetime, prepared devices with encapsulation were stored under an atmosphere with relative humidity of ~80% and temperature of ~25 °C. As shown in Figure 5, the PCE

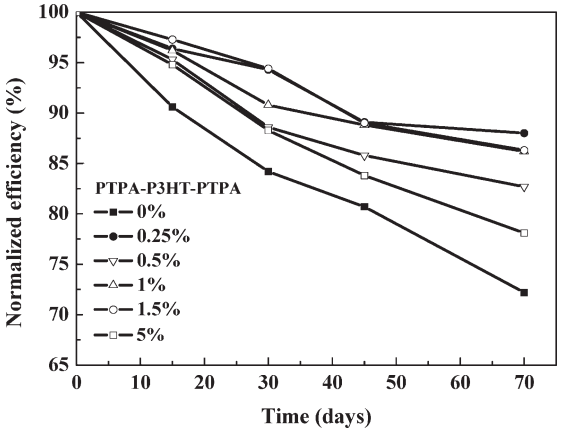

Figure 5. The lifetime of P3HT/PCBM (1:1, w/w) blended with 0%, 0.25%, 0.5%, 1%, 1.5%, and 5% of **PTPA-P3HT-PTPA** under air for 70 days.

Table 2. Photovoltaic Characteristics of P3HT/PCBM (1:1, w/w) Blended with Different Ratios of PTPA-P3HT-PTPA under 140 °C for 10 h for Thermal Stability Measurement

additives of PTPA-P3HT-PTPA under 140 °C for 10 h annealing (%)	J_{sc} (mA/cm^2)	V_{oc} (V)	FF (−)	PCE (%)	decay of PCE[a] (%)
0	6.4	0.65	0.55	2.3	41.2
1.5	8.5	0.62	0.62	3.3	24.7
5	8.1	0.62	0.62	3.1	24.9
10	7.5	0.63	0.6	2.8	10.2

[a] The PCE as compared to P3HT/PCBM (1:1) with different ratios of **PTPA-P3HT-PTPA** under 140 °C for 20 min annealing.

decays 28% in the case of pristine P3HT/PCBM (1:1) device after 70 days. Surprisingly, the addition of a surfactant could reduce the degradation ratio to be around 12−22% with various amounts of **PTPA-P3HT-PTPA** (0.25%-5%). The significantly enhanced environmental stability could be attributed to the increased tortuosity of the diffusion pathway[37] with the existence of a surfactant and to further reduction of the diffusion of oxygen and humidity into the internal part of the active layer.

Thermal annealing is a process to obtain BHJ morphology and to increase the mobility of P3HT in a solar cell system, but an excess of exposure to high temperatures leads to large-scale segregation of the two materials and devastation of the BHJ morphology.[7] The PCE of a pristine P3HT/PCBM device decays more than 40% upon 10 h of thermal treatment, compared to the normal conditions of 140 °C and 20 min as summarized in Table 2. The dramatic decrease of J_{sc} could be attributed to the PCBM aggregation effect inducing large-scale phase separation, which further reduces the interfacial area.[23] Apparently, the decay ratio of PCE was successfully suppressed to around 10−25% under long-term heating by the addition of **PTPA-P3HT-PTPA**. Furthermore, the optical microscopy images of the solar cells were explored to see the thermal effect on blended film as shown in Figure 6. For P3HT/PCBM blended with various amounts of **PTPA-P3HT-PTPA** (0%, 5%, and 10%) under 140 °C for 20 min, no obvious aggregates appeared in the optical microscopy images. With the long-term heating treatment, the needle-like aggregates of PCBM 150−350 μm in length dispersed densely in the pristine P3HT/PCBM system. Similar observations are reported for PCBM needles formed upon heating, attributed to a combination of local diffusion and crystallization of PCBM.[23] As for the 5% **PTPA-P3HT-PTPA**

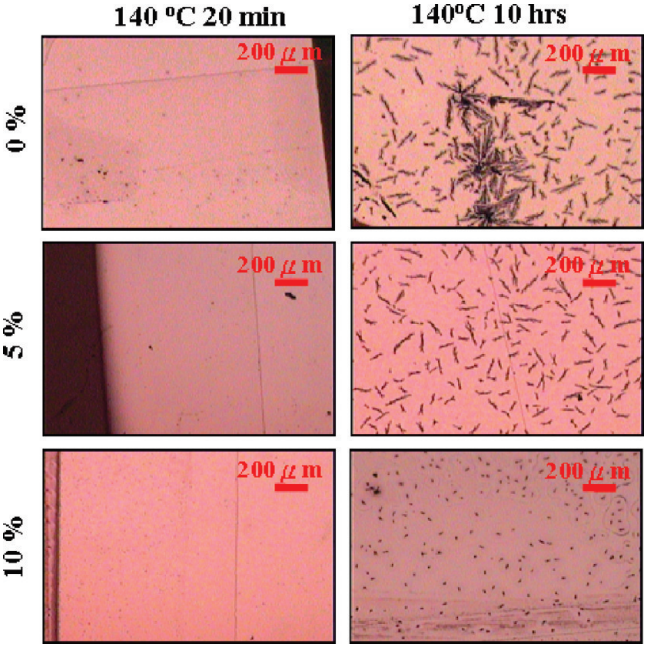

Figure 6. Optical microscopy images of P3HT/PCBM (1:1, w/w) blended with 0%, 5%, and 10% of **PTPA-P3HT-PTPA** under 140 °C for 20 min and 140 °C for 10 h.

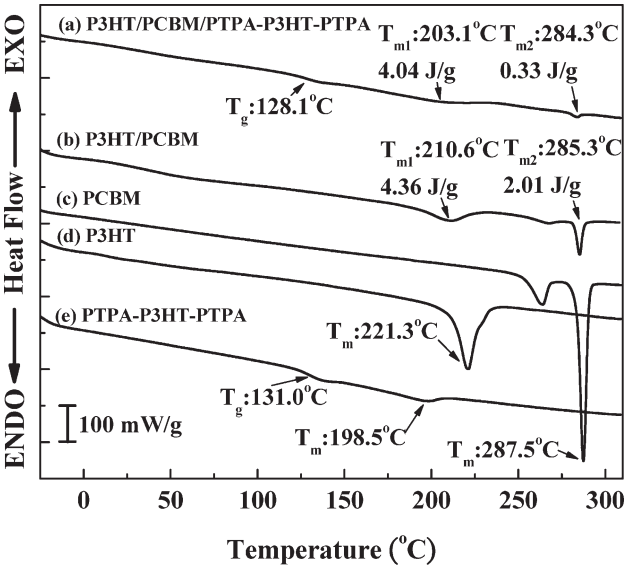

Figure 7. DSC curves of the (a) P3HT/PCBM/**PTPA-P3HT-PTPA**, (b) P3HT/PCBM, (c) PCBM, (d) P3HT, and (e) **PTPA-P3HT-PTPA** at the heating rate of 10 °C/min under a nitrogen atmosphere.

blend system, less dense PCBM aggregates and shorter needles (100−250 μm in length) were observed. Furthermore, the PCBM aggregation effects were significantly quenched (to 30−70 μm in length) when 10% **PTPA-P3HT-PTPA** was added. This suggested that the presence of a **PTPA-P3HT-PTPA** surfactant could stabilize the active-layer morphology against destructive thermal phase segregation.

DSC Study For Analyzing The Compatibilizing Effect. To further investigate the compatibilizing effect of **PTPA-P3HT-PTPA**, the phase transition behavior of pristine materials (P3HT, PCBM, and **PTPA-P3HT-PTPA**) and blend systems (P3HT/PCBM (3 mg/3 mg) and P3HT/PCBM/**PTPA-P3HT-PTPA** (3 mg/3 mg/6 mg)), such as the glass transition temperature (T_g), melting temperature

(T_m), and enthalpic changes upon melting, were estimated by differential scanning calorimetry (DSC) under thermal pretreatment conditions (10 °C/min for both heating and cooling scans), as shown in Figure 7. The distinct melting peaks of PCBM and P3HT were 287.5 and 221.3 °C in lines c and d, respectively. Also, **PTPA-P3HT-PTPA** (line e) exhibited T_g at 131.0 °C and T_m at 198.5 °C, which correspond to the contribution of the PTPA and P3HT segments, respectively. For the P3HT/PCBM (3 mg/3 mg) binary blended system (line b), the two melting peaks are assigned to the P3HT (T_{m1} = 210.6 °C) and PCBM (T_{m2} = 284.3 °C) melting characteristics in accordance with the corresponding pristine materials. With the addition of a surfactant to the ternary system (P3HT/PCBM/**PTPA-P3HT-PTPA**, 3 mg/3 mg/6 mg), three distinct peaks (T_g = 128.1 °C, T_{m1} = 203.1 °C, and T_{m2} = 284.3 °C) could be attributed to the PTPA segments of **PTPA-P3HT-PTPA**, pristine P3HT combined with the P3HT segment of **PTPA-P3HT-PTPA**, and pristine PCBM, respectively. The melting temperatures of the blend would decrease as compared to the individual components since the crystallinity and molecular arrangement were affected by each component. The broad endothermal melting peak of T_{m1} in the range of 158−240 °C maybe due to the broad molecular weight distribution of pristine P3HT (PDI ~2) and the formation of different crystal sizes of P3HT segments in the blend system. The enthalpic change of the P3HT segments in the binary system is 4.36 J/g, similar to that of the ternary system (4.04 J/g). However, the enthalpic change of PCBM in the ternary system (0.33 J/g) dramatically decreases compared to the binary system (2.01 J/g). These results indicate the selective miscibility of PTPA segments with PCBM, which suppress the large segregation of PCBM domains, maintaining the crystalline structure of P3HT domains. It is an important implication that large-scale phase separation and PCBM segregation upon annealing could be suppressed in the P3HT/PCBM blend system with the introduction of **PTPA-P3HT-PTPA**.

Conclusion

In summary, we have utilized a novel triblock copolymer, **PTPA-P3HT-PTPA**, comprised of poly(3-hexylthiophene) rod segment as a surfactant for P3HT/PCBM blend-based solar cells. With various amounts of **PTPA-P3HT-PTPA** added, the enhanced PCE could be related to the sphere-like nanostructure with enhanced interfacial area suitable for exciton dissociation and balanced mobility due to the donor characteristic of **PTPA-P3HT-PTPA**. The DSC measurement also help to explain the selective miscibility of PTPA coil segments with PCBM leading to the suppression of PCBM segregation upon annealing in accordance with optical microscopy study. The optimized PCE of the **PTPA-P3HT-PTPA** blended system reached up to 4.4% under illumination of AM 1.5G (100 mW/cm^2). This value is the highest among solar cell devices using block copolymers as surfactants. The increased PCE, combined with good air and thermal stability of solar cell devices by using a surfactant, indicates its promising potential for polymer solar cells.

Acknowledgment. The financial supports of National Science Council, Excellent Research Projects of National Taiwan University, and Ministry of Economic Affairs of Taiwan are highly appreciated.

Supporting Information Available: Text giving CV infromation and figures showing a ^{1}H NMR spectrum, CV plot, P-type and n-type transfer characteristics, and tapping mode AFM phase images for the P3HT/PCBM (1:1, w/w) with different ratios of **PTPA-P3HT-PTPA**. This material is available free of charge via the Internet at http://pubs.acs.org.

References and Notes

(1) Yu, G.; Gao, J.; Hummelen, J. C.; Wudl, F.; Heeger, A. J. *Science* **1995**, *270*, 1789.
(2) Li, G.; Yao, Y.; Yang, H.; Shrotriya, V.; Yang, G.; Yang, Y. *Adv. Funct. Mater.* **2007**, *17*, 1636.
(3) Peet, J.; Kim, J. Y.; Coates, N. E.; Ma, W. L.; Moses, D.; Heeger, A. J.; Bazan, G. C. *Nat. Mater.* **2007**, *6*, 497.
(4) Tsai, J. H.; Chueh, C. C.; Lai, M. H.; Wang, C. F.; Chen, W. C.; Ko, B. T.; Ting, C. *Macromolecules* **2009**, *42*, 1897.
(5) Chen, C. P.; Chan, S. H.; Chao, T. C.; Ting, C.; Ko, B. T. *J. Am. Chem. Soc.* **2008**, *130*, 12828.
(6) Li, G.; Shrotriya, V.; Huang, J. S.; Yao, Y.; Moriarty, T.; Emery, K.; Yang, Y. *Nat. Mater.* **2005**, *4*, 864.
(7) Yang, X. N.; Loos, J.; Veenstra, S. C.; Verhees, W. J. H.; Wienk, M. M.; Kroon, J. M.; Michels, M. A. J.; Janssen, R. A. J. *Nano Lett.* **2005**, *5*, 579.
(8) Chueh, C. C.; Higashihara, T.; Tsai, J. H.; Ueda, M.; Chen, W. C. *Org. Electron.* **2009**, *10*, 1541.
(9) Blouin, N.; Michaud, A.; Leclerc, M. *Adv. Mater.* **2007**, *19*, 2295.
(10) Kim, Y.; Cook, S.; Tuladhar, S. M.; Choulis, S. A.; Nelson, J.; Durrant, J. R.; Bradley, D. D. C.; Giles, M.; McCulloch, I.; Ha, C. S.; Ree, M. *Nat. Mater.* **2006**, *5*, 197.
(11) Li, Y. F.; Zou, Y. P. *Adv. Mater.* **2008**, *20*, 2952.
(12) Chang, Y. T.; Hsu, S. L.; Chen, G. Y.; Su, M. H.; Singh, T. A.; Diau, E. W. G.; Wei, K. H. *Adv. Funct. Mater.* **2008**, *18*, 2356.
(13) Xin, H.; Kim, F. S.; Jenekhe, S. A. *J. Am. Chem. Soc.* **2008**, *130*, 5424.
(14) Liang, Y. Y.; Wu, Y.; Feng, D. Q.; Tsai, S. T.; Son, H. J.; Li, G.; Yu, L. P. *J. Am. Chem. Soc.* **2009**, *131*, 56.
(15) Shaw, P. E.; Ruseckas, A.; Samuel, I. D. W. *Adv. Mater.* **2008**, *20*, 3516.
(16) Huijser, A.; Savenije, T. J.; Shalav, A.; Siebbeles, L. D. A. *J. Appl. Phys.* **2008**, *104*, 034505.
(17) Kim, Y.; Choulis, S. A.; Nelson, J.; Bradley, D. D. C.; Cook, S.; Durrant, J. R. *Appl. Phys. Lett.* **2005**, *86*, 063502.
(18) Sivula, K.; Ball, Z. T.; Watanabe, N.; Fréchet, J. M. J. *Adv. Mater.* **2006**, *18*, 206.
(19) Rajaram, S.; Armstrong, P. B.; Kim, B. J.; Fréchet, J. M. J. *Chem. Mater.* **2009**, *21*, 1775.
(20) Kim, K. C.; Park, J. H.; Park, O. O. *Sol. Energy Mater. Sol. Cells* **2008**, *92*, 1188.
(21) Yang, C.; Lee, J. K.; Heeger, A. J.; Wudl, F. *J. Mater. Chem.* **2009**, *19*, 5416.
(22) Lee, J. U.; Jung, J. W.; Emrick, T.; Russell, T. P.; Jo, W. H. *Nanotechnology* **2010**, *21*.
(23) Swinnen, A.; Haeldermans, I.; vande Ven, M.; D'Haen, J.; Vanhoyland, G.; Aresu, S.; D'Olieslaeger, M.; Manca, J. *Adv. Funct. Mater.* **2006**, *16*, 760.
(24) Sommer, M.; Lang, A. S.; Thelakkat, M. *Angew. Chem., Int. Ed.* **2008**, *47*, 7901.
(25) Sommer, M.; Huttner, S.; Steiner, U.; Thelakkat, M. *Appl. Phys. Lett.* **2009**, *95*, 183308.
(26) Sauve, G.; McCullough, R. D. *Adv. Mater.* **2007**, *19*, 1822.
(27) Iovu, M. C.; Zhang, R.; Cooper, J. R.; Smilgies, D. M.; Javier, A. E.; Sheina, E. E.; Kowalewski, T.; McCullough, R. D. *Macromol. Rapid Commun.* **2007**, *28*, 1816.
(28) Muller, C.; Goffri, S.; Breiby, D. W.; Andreasen, J. W.; Chanzy, H. D.; Janssen, R. A. J.; Nielsen, M. M.; Radano, C. P.; Sirringhaus, H.; Smith, P.; Stingelin-Stutzmann, N. *Adv. Funct. Mater.* **2007**, *17*, 2674.
(29) Li, B.; Sauve, G.; Iovu, M. C.; Jeffries-El, M.; Zhang, R.; Cooper, J.; Santhanam, S.; Schultz, L.; Revelli, J. C.; Kusne, A. G.; Kowalewski, T.; Snyder, J. L.; Weiss, L. E.; Fedder, G. K.; McCullough, R. D.; Lambeth, D. N. *Nano Lett.* **2006**, *6*, 1598.
(30) Radano, C. P.; Scherman, O. A.; Stingelin-Stutzmann, N.; Muller, C.; Breiby, D. W.; Smith, P.; Janssen, R. A. J.; Meijer, E. W. *J. Am. Chem. Soc.* **2005**, *127*, 12502.
(31) Higashihara, T.; Ohshimizu, K.; Hirao, A.; Ueda, M. *Macromolecules* **2008**, *41*, 9505.
(32) Higashihara, T.; Ueda, M. *Macromolecules* **2009**, *42*, 8794.
(33) Park, Y. D.; Lee, H. S.; Choi, Y. J.; Kwak, D.; Cho, J. H.; Lee, S.; Cho, K. *Adv. Funct. Mater.* **2009**, *19*, 1200.

(34) Morana, M.; Wegscheider, M.; Bonanni, A.; Kopidakis, N.; Shaheen, S.; Scharber, M.; Zhu, Z.; Waller, D.; Gaudiana, R.; Brabec, C. *Adv. Funct. Mater.* **2008**, *18*, 1757.
(35) Campoy-Quiles, M.; Ferenczi, T.; Agostinelli, T.; Etchegoin, P. G.; Kim, Y.; Anthopoulos, T. D.; Stavrinou, P. N.; Bradley, D. D. C.; Nelson, J. *Nat. Mater.* **2008**, *7*, 158.
(36) Chiu, M. Y.; Jeng, U. S.; Su, M. S.; Wei, K. H. *Macromolecules* **2010**, *43*, 428.
(37) Prattipati, V.; Hu, Y. S.; Bandi, S.; Schiraldi, D. A.; Hiltner, A.; Baer, E.; Mehta, S. *J. Appl. Polym. Sci.* **2005**, *97*, 1361.
(38) Bao, Z.; Locklin, J. *Organic field-effect transistors*; CRC Press: Boca Raton, FL, 2007.
(39) Iovu, M. C.; Jeffries-El, M.; Zhang, R.; Kowalewski, T.; McCullough, R. D. *J. Macromol. Sci. Pure Appl. Chem.* **2006**, *43*, 1991.
(40) Liu, J.; Sheina, E.; Kowalewski, T.; McCullough, R. D. *Angew. Chem., Int. Ed.* **2002**, *41*, 2.